

Temperature dependence of the intrinsic anomalous Hall effect in nickel

Li Ye, Yuan Tian, and Xiaofeng Jin*

State Key Laboratory of Surface Physics and Department of Physics, Fudan University, Shanghai 200433, China

Di Xiao

Materials Science and Technology Division, Oak Ridge National Laboratory, Oak Ridge, Tennessee 37831, USA

(Received 28 May 2011; revised manuscript received 6 March 2012; published 19 June 2012)

The unusual temperature dependence of the anomalous Hall effect (AHE) in Ni is investigated by an experimental approach which enables us to extract the intrinsic anomalous Hall conductivity over the whole temperature range. In stark contrast to the existing literature, the intrinsic contribution in Ni is found to be strongly temperature dependent between 5 and 150 K, where the corresponding magnetization remains almost unchanged. This pronounced temperature dependence, a cause of the long-standing confusion concerning the physical origin of the AHE in Ni, is likely due to the existence of small band gaps caused by the spin-orbit coupling at the Fermi level. Our result helps pave the way for the general claim of the Berry-phase interpretation for the AHE, and also points out another mechanism for the temperature dependence of the AHE.

DOI: [10.1103/PhysRevB.85.220403](https://doi.org/10.1103/PhysRevB.85.220403)

PACS number(s): 72.15.Eb, 71.70.Ej, 73.50.Jt, 75.47.Np

Recent years have seen a surge of renewed interest in the anomalous Hall effect (AHE) in ferromagnets, largely driven by its close relationship to various spintronic applications.¹ A major challenge in this field is to clarify the microscopic origin of the AHE, which has been a controversial subject for more than half a century. It is now recognized that there are several competing mechanisms. One is the extrinsic mechanism based on the modified impurity scattering in the presence of the spin-orbit coupling (SOC), i.e., the skew scattering and the side-jump mechanisms.^{2,3} The other stems from the anomalous velocity of Bloch electrons induced by the SOC, originally proposed by Karplus and Luttinger.⁴ This latter contribution can be interpreted as the Berry curvature of the occupied Bloch states and is of an intrinsic nature.⁵⁻⁷ Based on recent experiments and theoretical calculations, the physical picture of two limiting cases has emerged: The skew scattering contribution is the most significant in ultrapure samples at low temperatures,⁸ while the intrinsic contribution dominates in moderately conducting samples at high temperatures.⁹⁻¹² However, what happens in between, and particularly the temperature dependence of the AHE, is still unclear and remains a challenge in both experimental and theoretical studies.

In this Rapid Communication, we propose a general experimental method that can be used to distinguish various contributions to the AHE across the *entire* temperature range, using Ni as an example. Our approach involves the manipulation of mask and shadow in the molecular beam epitaxy chamber,^{13,14} which allows us to integrate *in situ*, on a single substrate, a series of stepped Ni films with well-controlled thicknesses (d), as shown in Fig. 1(a). By establishing the scaling between the anomalous Hall resistivity ρ_{AH} and the longitudinal resistivity $\rho_{xx}(d)$ at different temperatures,¹⁵ we are able to extract the intrinsic anomalous Hall conductivity in Ni. Our result reveals a dominant intrinsic contribution to the AHE at high temperatures, which agrees with other transition metal ferromagnets such as Fe and Co.^{11,16-18} Surprisingly, we find that the intrinsic AHE is strongly temperature dependent over a large range (5–150 K) in which the magnetization stays almost

the same. Specifically, the intrinsic term at low temperature is almost two times larger than its room-temperature value. This is puzzling because the intrinsic AHE is regarded as a ground state property and should not change much when the temperature is well below the Curie temperature. We attribute this pronounced temperature dependence to the existence of small band gaps caused by the spin-orbit coupling at the Fermi level. Our result not only paves the way for the general claim of the Berry-phase interpretation for the AHE, but also points out another important yet general mechanism for the temperature dependence of the AHE.

A clean and ordered MgO(001) surface was first prepared by annealing at 1100 K in ultrahigh vacuum (UHV), on which the epitaxial growth of Ni at 300 K was then followed. It was further annealed at 600 K for 1 h to acquire better crystal quality and surface morphology. A representative reflection high energy electron diffraction (RHEED) pattern after annealing is shown in the inset of Fig. 1(a). The improved sample quality after the annealing was also revealed from the significant decrease (>50%) of the corresponding sample residual resistivity ρ_{xx0} . Meanwhile, the magnetization monitored by *in situ* magneto-optic Kerr effect (MOKE) measurements¹³ remained almost the same, indicating that the oxide formation between Ni and MgO was negligible, in agreement with the previous results in literature.¹⁹ In addition, a direct comparison of the RHEED intensity line profiles of MgO(001) and Ni(001) indicated that Ni films ≥ 6 nm have the same lattice constant of bulk Ni (0.352 nm), also in agreement with literature.¹⁹ Finally, in order to prevent oxidation in the ambient air during the transport measurement, a capping layer of 5 nm MgO was deposited on top of Ni before each sample was taken out from the UHV chamber. The films were then patterned into standard Hall bars along [100] for the transport measurement, with the magnetic field applied along [001].

Figure 1(a) shows the residual resistivity ρ_{xx0} of Ni (measured at 5 K) as a function of film thickness ranging from 6 to 30 nm, where a fivefold decrease is observed. This is due to the finite size effect in electrical resistivity of thin metallic films induced by the geometrical limitation of the bulk (or

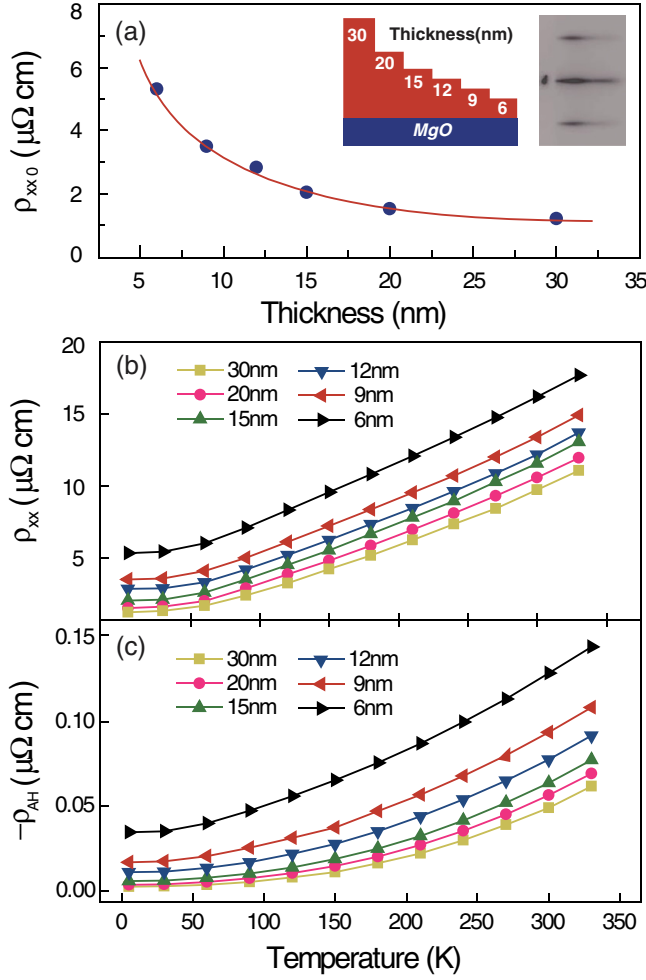


FIG. 1. (Color online) (a) Thickness dependence of ρ_{xx0} in Ni thin films. The red (solid) line is a guide for the eyes. Insets: Side view of the sample, and RHEED pattern for 30 nm Ni film. (b), (c) Temperature dependence of ρ_{xx} and ρ_{AH} for various film thicknesses.

background) mean free path of conduction electrons.²⁰ The current selection of film thicknesses (6–30 nm) allows us to change the impurity scattering with little alternation of the bulk electronic structure.^{21,22} Figures 1(b) and 1(c) show the temperature dependence of both ρ_{xx} and ρ_{AH} for different film thicknesses, respectively. The negative sign of ρ_{AH} reflects the fact that the chirality of the AHE in Ni is opposite to that of Fe.²³ We plot ρ_{AH} as a function of ρ_{xx} for the thickest (30 nm Ni) film using the logarithmic scale in Fig. 2(a). The $\rho_{AH} = f(\rho_{xx})$ curve agrees well with previous observations for the temperature-dependent scaling of the AHE in bulk Ni.²⁴ It is exactly this complicated temperature-dependent scaling that makes the intrinsic origin of the AHE in Ni rather elusive.

As an attempt, we now try to separate the different contributions to the AHE by applying the scaling law proposed in our previous work:¹¹

$$\sigma_{AH} = -(\alpha\sigma_{xx0}^{-1} + \beta\sigma_{xx0}^{-2})\sigma_{xx}^2 - b, \quad (1)$$

where α , β , and b are constants to be determined, and σ_{AH} , σ_{xx0} , and σ_{xx} are the anomalous Hall conductivity, and residual

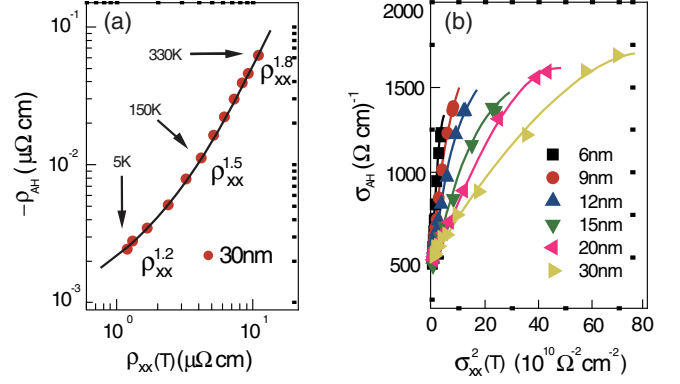


FIG. 2. (Color online) (a) Temperature-dependent power law between ρ_{AH} and $\rho_{xx}(T)$ for 30 nm Ni film. (b) σ_{AH} vs $\sigma_{xx}^2(T)$ plot for various film thicknesses.

and total longitudinal conductivities, respectively. Here, the first and last terms represent the extrinsic skew scattering (σ_{sk}) and the intrinsic Berry phase (σ_{int}) contributions, respectively. Similar to the first term, the β term is clearly of extrinsic origin, and was previously ascribed to the side-jump contribution. Figure 2(b) shows σ_{AH} as a function of $\sigma_{xx}^2(T)$ from 5 to 330 K for different film thicknesses. It is observed, as anticipated, that when $\sigma_{xx}^2(T)$ goes to zero, the anomalous Hall conductivity σ_{AH} for various film thicknesses with different residual resistivity converges to a universal value of $500 \Omega^{-1} \text{ cm}^{-1}$, reflecting unambiguously the intrinsic nature of the AHE at the high temperature limit. However, for a given thickness, a significant deviation from a linear scaling between σ_{AH} and $\sigma_{xx}^2(T)$ is clearly noticeable, suggesting that the scaling in Eq. (1) does not apply to the AHE in Ni, if α , β , and b were to be fixed as temperature-independent constants.

To remedy the above difficulty, we propose now a generic scaling

$$\sigma_{AH} = -(\alpha\sigma_{xx0}^{-1} + \beta\sigma_{xx0}^{-2})\sigma_{xx}^2 - b(T), \quad (2)$$

or equivalently

$$\rho_{AH} = (\alpha\rho_{xx0} + \beta\rho_{xx0}^2) + b(T)\rho_{xx}^2, \quad (3)$$

where α and β are still constants, but $b(T)$, which represents the intrinsic Berry-phase contribution, is now a function of temperature. Our assumption that the intrinsic contribution $b(T)$ might be temperature dependent is motivated by the fact that the magnetocrystalline anisotropy of Ni is strongly temperature dependent between 5 and 330 K.²⁵ Since the Berry-phase contribution to the AHE originates from the same SOC effect in the band structure, it is natural to expect that it could also be temperature dependent. Therefore, instead of analyzing the scaling $\rho_{AH} = f[\rho_{xx}(T)]$ with varying temperature for each fixed film thickness, we should consider the same scaling but with varying film thicknesses for each fixed temperature $\rho_{AH} = f[\rho_{xx}(d)]$.

We first consider the low-temperature limit. Because of the Matthiessen rule, the scaling Eq. (3) at 5 K reduces to $\rho_{AH0} = \alpha\rho_{xx0} + (\beta + b_0)\rho_{xx0}^2$, where $b_0 = b(T = 5 \text{ K})$ is a constant for different film thicknesses. From the linear fitting to the $\rho_{AH0}/\rho_{xx0}(d)$ vs $\rho_{xx0}(d)$ plot as shown in Fig. 3(a)

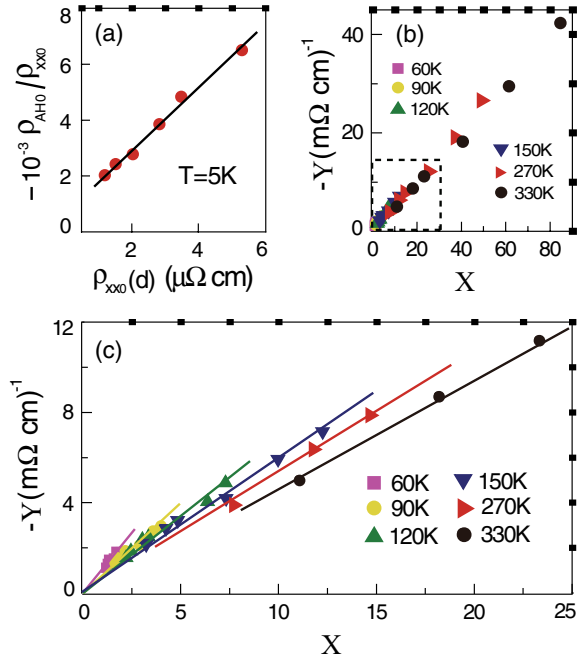


FIG. 3. (Color online) (a) ρ_{AH0}/ρ_{xx0} vs ρ_{xx0} plot. (b) Y vs X plot at various temperatures. (c) Zoom-in plot of the dashed box of (b).

and using the set of 5 K data in Figs. 1(b) and 1(c), we obtain the skew scattering constant $\alpha = -7 \times 10^{-4}$ from the intercept, which is noticeably smaller than $\alpha = -3.7 \times 10^{-3}$ in the Fe/GaAs(001) case.¹¹

Now Eq. (3) can be recast into $Y = b(T)X + \beta$, where $Y = (\rho_{AH} - \alpha\rho_{xx0})/\rho_{xx0}^2$ and $X = \rho_{xx}^2/\rho_{xx0}^2$. For each fixed temperature (ranging from 5 to 330 K), we show in Fig. 3(b) a plot of Y vs X with varying film thickness d . It is clear from Fig. 3(c) [zoom-in part in Fig. 3(b)] that at each given temperature all the experimental data can indeed be well described by the generic scaling, as they can be fitted by the straight lines in the whole temperature range. In addition, all the lines pass the origin, indicating the fact that $\beta \approx 0$. Note that both α and β in Ni/MgO(001) are significantly smaller than those in Fe/GaAs(001),¹¹ which could be either due to the different extrinsic scatters in Ni and Fe, or caused by the dominant interface scattering for the electrical resistivity in ultrathin films,^{20,26} where the SOC is known to be significantly smaller for MgO (light elements) than GaAs (heavy elements).

The slopes in Fig. 3(c) at different temperatures give the intrinsic temperature-dependent anomalous Hall conductivity $\sigma_{int}(T) = -b(T)$ in Ni, which are shown in Fig. 4, marked by solid green circles. $\sigma_{int}(T)$ is about $1100 (\Omega \text{ cm})^{-1}$ at 5 K, and decreases to about $500 (\Omega \text{ cm})^{-1}$ at 300 K. It is obvious that this temperature-dependent term $\sigma_{int}(T)$ cannot be singled out from the AHE measurements on a single Ni sample. Instead, it is only possible on a series of samples with tunable residual resistivity ρ_{xx0} while keeping their electronic band structures basically the same (otherwise the corresponding intrinsic contributions would be different from each other). Now it becomes transparent that it is this temperature-dependent intrinsic term that has caused earlier complications and confusions in understanding the AHE in Ni.

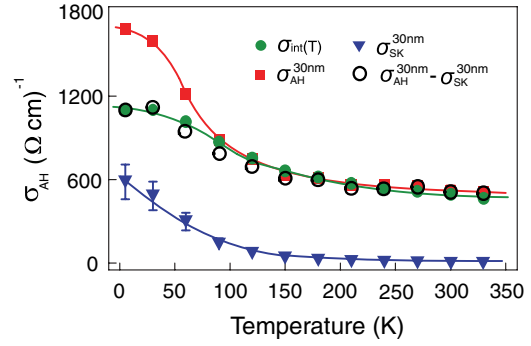


FIG. 4. (Color online) The temperature-dependent σ_{int} (green, solid circle) in Ni together with various contributions extracted from 30 nm thick Ni. The solid curves are guide for the eyes.

To better understand the microscopic mechanisms of the AHE in bulk Ni, we also show in Fig. 4 the data (red square dots) of the experimentally measured anomalous Hall conductivity $\sigma_{AH}^{30 \text{ nm}}$ in the bulklike 30 nm thick Ni film. Using the aforementioned result of $\alpha = -7 \times 10^{-4}$ we can also plot the temperature-dependent skew scattering conductivity $\sigma_{sk}^{30 \text{ nm}} = -\alpha\sigma_{xx0}^{-1}\sigma_{xx}^2(T)$ for this bulklike 30 nm Ni film, shown as blue triangles in Fig. 4. Now subtracting $\sigma_{sk}^{30 \text{ nm}}$ from $\sigma_{AH}^{30 \text{ nm}}$, we obtain the intrinsic anomalous Hall conductivity in this 30 nm Ni film, as given by the open circles in Fig. 4. It should be emphasized that $\sigma_{int}(T)$ and $\alpha = -7 \times 10^{-4}$ are obtained from a series of samples with different film thicknesses (not necessary to include the data from the 30 nm Ni film) while $\sigma_{AH}^{30 \text{ nm}} - \sigma_{sk}^{30 \text{ nm}}$ is for a single film thickness. The excellent agreement between $\sigma_{int}(T)$ and $\sigma_{int}^{30 \text{ nm}}$ clearly reflects the consistency of the overall analysis adopted here. In addition, it can be seen clearly from Fig. 4 that the intrinsic contribution dominates in the whole temperature range from 5 to 300 K.

In previous studies, the temperature dependence of the intrinsic AHE is explained by the temperature dependence of the magnetization.^{27,28} However, this argument obviously does not work here because the Curie temperature of 4 nm thick Ni film is already close to 600 K;²¹ the minor magnetization change (<10%) below 150 K cannot possibly explain the significant temperature dependence of $\sigma_{int}(T)$. We propose that such a strong temperature dependence can be associated with the Fermi energy passing through small band gaps caused by the SOC. Typically, around such small band gaps the Berry curvature of the occupied and unoccupied bands has opposite signs and is highly concentrated at the anticrossing point.^{1,7} As the temperature increases, the bottom of the unoccupied bands will be thermally populated, which has a cancellation effect on the anomalous Hall conductivity (AHC). Once these states with concentrated Berry curvatures are fully populated, a further increase in temperature will have little effect on the AHC. We therefore expect that the absolute value of the AHC will first decrease then saturate as the temperature increases. This trend is observed in Fig. 4. In fact, the mechanism of thermal population of empty bands immediately above the Fermi level was exactly the clue to explain the aforementioned temperature dependence of the magnetocrystalline anisotropy of Ni.^{29,30} In addition, a similar cancellation effect of the Berry curvature has also been predicted in first-principles calculation of the spin Hall effect in Pt.³¹ While the effect of magnon

scattering cannot be completely ruled out, its role is rather small in the temperature range studied in our experiment.³²

With our insight on the AHE in Ni, we now clarify the earlier confusions and complications in literatures. Given the values of $\sigma_{\text{int}}(5\text{ K}) = 1100\ (\Omega\text{ cm})^{-1}$ and $\alpha = -7 \times 10^{-4}$, the skew scattering term $\rho_{\text{sk}} = \alpha\rho_{xx0}$ is expected to overwhelm the intrinsic one $\rho_{\text{int}} = -\sigma_{\text{int}}\rho_{xx}^2$ if the residual resistivity ρ_{xx0} is below $0.5\ \mu\Omega\text{ cm}$, which corresponds to the so-called “clean limit” in the AHE where the linear term $\rho_{\text{AH0}} = \alpha\rho_{xx0}$ dominates. This explains why in the ultrapure Ni samples at low temperature, Fert *et al.* did observe an overall linear scaling $\rho_{\text{AH0}} = \alpha\rho_{xx0}$.⁸ On the other hand, the temperature-dependent power law scaling ρ_{xx}^n is in fact some ill-defined average of the real scaling $\rho_{\text{AH}} = \alpha\rho_{xx0} + \beta\rho_{xx0}^2 - \sigma_{\text{int}}(T)\rho_{xx}^2$. Finally, so far first-principles calculations of the intrinsic AHE have been compared to $320\text{--}750\ (\Omega\text{ cm})^{-1}$ measured at room temperature.^{2,24} Our result shows that for zero-

temperature calculations, one should compare to $\sigma_{\text{int}}(5\text{ K}) = 1100\ (\Omega\text{ cm})^{-1}$.

Recently we became aware of two theoretical studies of the AHE in Ni. Based on a generalized gradient approximation (GGA) + U calculation, it was shown that when the exchange splitting is tuned to the experimental value, $\sigma_{\text{int}} = 1200\ (\Omega\text{ cm})^{-1}$, close to our experimental data at 5 K.³³ In another study the authors have confirmed and expanded our explanation of the temperature-dependent intrinsic AHE.³⁴

The authors thank G. Malcolm Stocks for useful discussions on the band structure of Ni. This work was supported by MOST (No. 2009CB929203), NSFC (No. 10834001), and SCST. D.X. acknowledges support from the US Department of Energy, Office of Basic Energy Sciences, the Division of Materials Sciences and Engineering.

*Corresponding author: xfjin@fudan.edu.cn

¹N. Nagaosa *et al.*, *Rev. Mod. Phys.* **82**, 1539 (2010).

²J. Smit, *Physica (Amsterdam)* **21**, 877 (1955).

³L. Berger, *Phys. Rev. B* **2**, 4559 (1970).

⁴R. Karplus and J. M. Luttinger, *Phys. Rev.* **95**, 1154 (1954); J. M. Luttinger, *ibid.* **112**, 739 (1958).

⁵T. Jungwirth, Q. Niu, and A. H. MacDonald, *Phys. Rev. Lett.* **88**, 207208 (2002).

⁶M. Onoda *et al.*, *J. Phys. Soc. Jpn.* **71**, 19 (2002).

⁷D. Xiao *et al.*, *Rev. Mod. Phys.* **82**, 1959 (2010).

⁸A. Fert *et al.*, *Phys. Rev. Lett.* **28**, 303 (1972).

⁹S. Onoda, N. Sugimoto, and N. Nagaosa, *Phys. Rev. Lett.* **97**, 126602 (2006).

¹⁰T. Miyasato, N. Abe, T. Fujii, A. Asamitsu, S. Onoda, Y. Onose, N. Nagaosa, and Y. Tokura, *Phys. Rev. Lett.* **99**, 086602 (2007).

¹¹Y. Tian, L. Ye, and X. Jin, *Phys. Rev. Lett.* **103**, 087206 (2009).

¹²Z. Fang *et al.*, *Science* **302**, 92 (2003).

¹³L. F. Yin, D. H. Wei, N. Lei, L. H. Zhou, C. S. Tian, G. S. Dong, X. F. Jin, L. P. Guo, Q. J. Jia, and R. Q. Wu, *Phys. Rev. Lett.* **97**, 067203 (2006).

¹⁴C. S. Tian *et al.*, *Phys. Rev. Lett.* **94**, 137210 (2005).

¹⁵This is different from our previous study of the AHE in Fe (Ref. 11), in which the focus is on the scaling between ρ_{AH} and $\rho_{xx}(T)$ at different film thicknesses.

¹⁶X. Wang, D. Vanderbilt, J. R. Yates, and I. Souza, *Phys. Rev. B* **76**, 195109 (2007).

¹⁷Y. Yao, L. Kleinman, A. H. MacDonald, J. Sinova, T. Jungwirth, D. S. Wang, E. Wang, and Q. Niu, *Phys. Rev. Lett.* **92**, 037204 (2004).

¹⁸E. Roman, Y. Mokrousov, and I. Souza, *Phys. Rev. Lett.* **103**, 097203 (2009).

¹⁹A. Barbier *et al.*, *J. Appl. Phys.* **84**, 4259 (1998).

²⁰C. R. Tellier and A. J. Tosser, *Size Effects in Thin Films* (Elsevier, Amsterdam, 1982).

²¹R. J. Zhang and R. F. Willis, *Phys. Rev. Lett.* **86**, 2665 (2001).

²²M. Hoesch, V. N. Petrov, M. Muntwiler, M. Hengsberger, J. L. Checa, T. Greber, and J. Osterwalder, *Phys. Rev. B* **79**, 155404 (2009).

²³*The Hall Effect and Its Applications*, edited by C. L. Chien and C. R. Westgate (Plenum, New York, 1980).

²⁴J. M. Lavine, *Phys. Rev.* **123**, 1273 (1961).

²⁵W. J. Carr, *Phys. Rev.* **109**, 1971 (1958).

²⁶T. Hirahara *et al.*, *Appl. Phys. Lett.* **91**, 202106 (2007).

²⁷R. Mathieu, A. Asamitsu, H. Yamada, K. S. Takahashi, M. Kawasaki, Z. Fang, N. Nagaosa, and Y. Tokura, *Phys. Rev. Lett.* **93**, 016602 (2004).

²⁸C. Zeng, Y. Yao, Q. Niu, and H. H. Weitering, *Phys. Rev. Lett.* **96**, 037204 (2006).

²⁹W. N. Furey, Ph.D. thesis, Harvard University, 1967.

³⁰E. I. Kondorskii *et al.*, *Sov. Phys. JETP* **36**, 188 (1973); E. I. Kondorskii and E. Straube, *Zh. Eksp. Teor. Fiz.* **63**, 356 (1972).

³¹G. Y. Guo, S. Murakami, T. W. Chen, and N. Nagaosa, *Phys. Rev. Lett.* **100**, 096401 (2008).

³²S. A. Yang, H. Pan, Y. Yao, and Q. Niu, *Phys. Rev. B* **83**, 125122 (2011).

³³H. R. Fuh and G. Y. Guo, *Phys. Rev. B* **84**, 144427 (2011).

³⁴A. Shitade and N. Nagaosa, [arXiv:1109.5463](https://arxiv.org/abs/1109.5463).